Conceptual Study of Aero-Gravity Assist Trajectory Using Earth's Atmosphere

Jun NAKAYA (National Institute of Technology, Gifu College)

Abstract

Aero-gravity assist is a future orbital technique proposed by Lewis et al. This technique is realized by a spacecraft with a high lift-to-drag ratio flying upside down in the planetary atmosphere. Aero-gravity assist is expected to accelerate beyond gravity assist. However, detailed analyses, such as numerically solving the spacecraft motion, have not been done. Therefore, in this study, by numerically solving the three-degree-of-freedom movement of the spacecraft, the acceleration, the nose temperature, and the entry corridor of the spacecraft obtained by aero-gravity assist are estimated. Based on the results, the effectiveness of aero-gravity assist can be investigated.

地球大気を利用した重力ー空力アシスト軌道の概念検討

中谷　淳　（岐阜工業高等専門学校）

摘要

重力ー空力アシストはMark J. Lewisらによって提案された将来の軌道技術である。この技術は高い揚抗比の宇宙機が惑星大気圏内を背面飛行することによって実現される。重力ー空力アシストは重力アシスト以上の加速が期待されている。しかし、現在までに宇宙機の運動を数値的に解くなどの詳細な解析は実施されていない。そこで、本研究では宇宙機の三自由度運動を数値的に解くことにより、重力ー空力アシストで得られる宇宙機の加速量、機首温度、j突入回廊を推算する。得られた結果を踏まえ、重力ー空力アシストの有効性を評価する。

1. Introduction

Gravity assist is an indispensable orbital technique for solar system exploration. The gravity assist enables the spacecraft to maneuver without the consumption of propellant by utilizing the universal gravitation and revolution of the planet. The outline of gravity assist is shown in Fig. 1, and the acceleration ΔV obtaind by gravity assist is shown by Eq. (1). In addition, gravity assist has strong constraint conditions, expressed by the Eq. (2), and the three variables of the closest approach altitude, deflection angle, and hyperbolic excess velocity are associated.

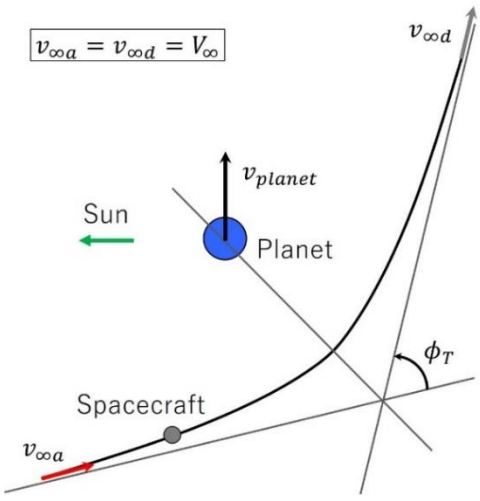

Fig. 1.　Outline of the gravity assist

$$\Delta V = 2V_\infty \cos\frac{\phi_T}{2} \quad (1)$$

$$\sin\frac{\phi_T}{2} = \frac{1}{\frac{V_\infty^2(R+h)}{\mu}+1} \quad (2)$$

Fig. 2. shows the relationship between the acceleration and the deflection angle, and the acceleration obtained with the deflection angle increase also increases. In addition, Fig. 3 shows the relationship between the closest approach altitude and the deflection angle, and the deflection angle increases as the closest approach altitude decreases. However, because it is necessary to consider the size of the planet and the atmosphere, the amount of acceleration obtained by gravity assist is limited.

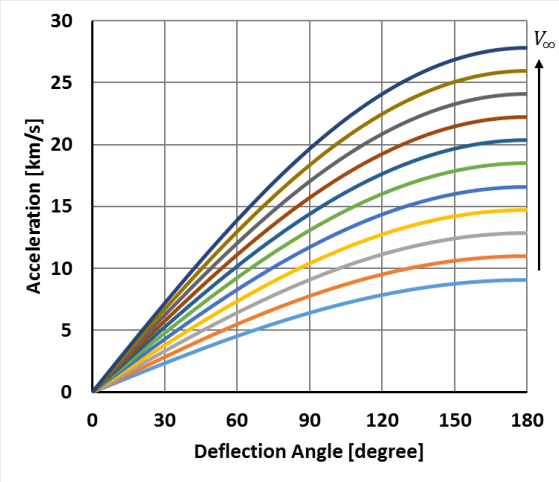

Fig. 2. Relationship between acceleration and deflection angle

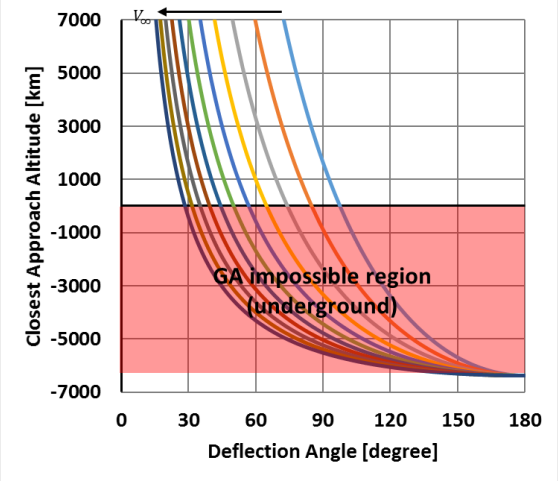

Fig. 3. Relationship between closest approach altitude and deflection angle

In this study, aero-gravity assist, proposed by Lewis et al. as a technique for obtaining further acceleration with gravity assist, is addressed. According to Lewis et al., a spacecraft with a high lift-to-drag ratio ($L/D > 5$) will fly upside down in a planetary atmosphere, resulting in acceleration beyond gravity assist[1)]. Waverider is expected to be a spacecraft shape that realizes high lift-to-drag ratio. The flight model of Lewis et al. is shown in Fig. 4.

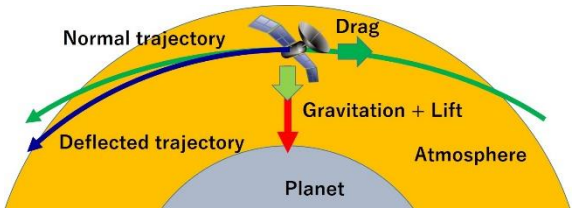

Fig. 4. Flight model of the aero-gravity assist

When assessing the effectiveness of aero-gravity assist, the most important consideration is whether the spacecraft can accelerate beyond gravity assist. However, complicated factors, such as the aerodynamic heating and thermal protection system accompanying atmospheric flight, as well as the relationship between the width of the entry corridor and the controllability of the spacecraft, need to be studied in detail. Specific items that affect the effectiveness of aero-gravity assist are as follows.

(a) Approach conditions to the planet (approach speed, flight path angle, azimuth, closest approach altitude)

(b) Specifications of the spacecraft (drag coefficient, lift coefficient, wing area, nose radius)

(c) Attitude of the spacecraft (pitch angle, roll angle, yaw angle)

Detailed analysis of aero-gravity assist has not yet been done. In addition, it is difficult to develop a spacecraft with a lift-to-drag ratio of 5.0 or higher from the viewpoint of technology readiness level. Therefore, in this study, a spacecraft with a lift-to-ratio of 5.0 or less is subject to analysis. It is also supposed to fly in the Earth's atmosphere. Numerically solving the three-degree-of-freedom motion of the spacecraft makes it possible to estimate the amount of acceleration of the spacecraft, nose

temperature, and entry corridor in aero-gravity assist. Considering the obtained results makes it possible for the effectiveness of aero-gravity assist to be evaluated.

2. Analysis method

The analysis coordinate system is a polar coordinate system whose origin is Earth's center, the reference direction is the direction of the spacecraft at the start of calculation, and the reference plane is the equatorial plane (Fig. 5).

The three-degree-of-freedom motion of the spacecraft is shown in Eq. (3). The force on the spacecraft is the universal gravitation of the earth and the aerodynamic force (drag and lift) received from the atmosphere. The atmospheric data use the density, atmospheric pressure, and temperature of the standard atmosphere. In addition, it is possible to consider the attitude of the spacecraft, which changes every minute. Eq. (3) is solved by the Runge–Kutta–Fehlberg formula. The area to calculate the trajectory of the spacecraft is within the sphere of influence of Earth. The radius of the sphere of influence is calculated by Eq. (4).

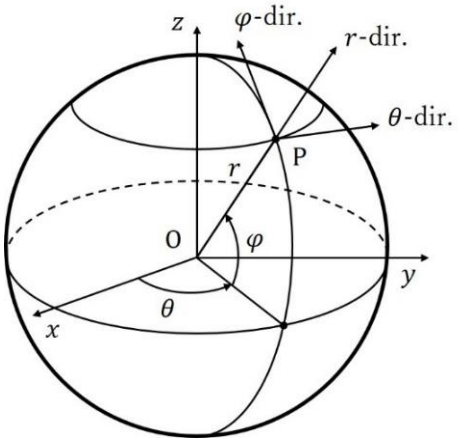

Fig. 5. Coordinate system

$$m\frac{d^2\vec{r}}{dt^2} = m\frac{\mu}{\vec{r}^2} + C_D\frac{1}{2}\rho\vec{u}^2S + C_L\frac{1}{2}\rho\vec{u}^2S \quad (3)$$

$$R_s = R\left(\frac{M_{planet}}{M_{sun}}\right)^{\frac{2}{5}} \quad (4)$$

The nose temperature of the spacecraft is estimated by the radiation equilibrium condition between the aerodynamic heating amount of the nose stagnation point obtained by the Detra–Kemp–Riddell formula in Eq. (5)[2] and the radiation heat quantity obtained by the Stefan–Boltzmann law in Eq. (6). Here, the total hemispherical emissivity ε is 0.95, assuming that carbon is used for thermal protection.

$$\dot{q}_w = \frac{110.35}{\sqrt{R_0}}\sqrt{\frac{\rho_\infty}{\rho_{SL}}}\left(\frac{V_\infty}{V_C}\right)^{3.15}\left(\frac{h_s - h_w}{h_s - h_{300}}\right) \quad (5)$$

$$\dot{q}_{rad} = \varepsilon\sigma T^4 \quad (6)$$

3. Analysis Conditions

The analysis conditions are shown in Table 1.

Table 1. Analysis conditions

(a) Approach conditions to the planet	
Initial flight velocity	A multiple of the second cosmic velocity converted into a value at the sphere of influence
Closest approach altitude	100 km (max) 40 km (min)
(b) Specifications of the spacecraft (modeling from Hayabusa 2)	
Mass	500 kg
Wing area	10 m^2 (refer to the area of solar panels)
Drag coefficient	0.5 (approximate value by CFD analysis)
Lift-to-drag ratio	5.0, 1.0, 0.1, 0.01
Nose radius	1 m (unit length)
(c) Attitude control of the spacecraft during the atmospheric flight	
Roll angle	-180° (upside down) 0° (normal)

In this analysis, initial velocity, closest approach altitude, lift-to-drag ratio, and roll angle are changed parametrically and given as initial conditions. The initial speed is set as the multiple (5–10 times) by converting the second cosmic velocity (11.18 km/s) into the velocity of the boundary of the sphere of influence. The closest approach altitude is given in increments of 1 km

within the range of 100 to 40 km. For the drag coefficient, the shape of the modeled Hayabusa 2 is set as a reference value for hypersonic flight using the high-speed fluid analysis tool FaSTAR[3]. Based on the obtained drag coefficient, by changing the lift coefficient, four lift-to-drag ratios of 5.0, 1.0, 0.1, and 0.01 are given. The attitude of the spacecraft gives only the roll angle of 180° (default, upside-down flight), or 0° (normal flight).

4. Results and discussion

Figs. 6-9 show the relationship between the closest approach altitude and acceleration obtained by the aero-gravity assist calculation, whose initial approach speeds are multiples of seven, eight, nine, and ten times. The roll angle is -180° for all. Fig. 6 shows that the acceleration obtained with the speed multiple of seven is smaller than that of the gravity assist. That is, in the case of speed multiple seven, there is no effect of aero-gravity assist. In the case of speed multiple eight, the acceleration attained by aero-gravity assist is greater than the gravity assist at the closest altitude of 80 km or less. In the case of speed multiples nine and ten, the acceleration obtained by the aero-gravity assist is increased more than that by the gravity assist. The difference in lift-to-drag ratio affects only the closest approach altitude, as shown in these figures.

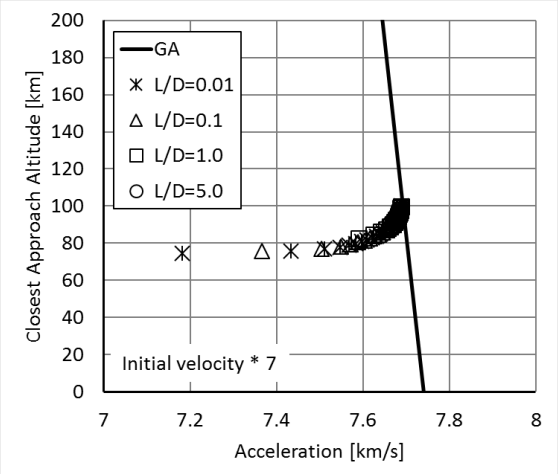

Fig. 6. Relationship between the closest altitude and acceleration (speed multiple 7)

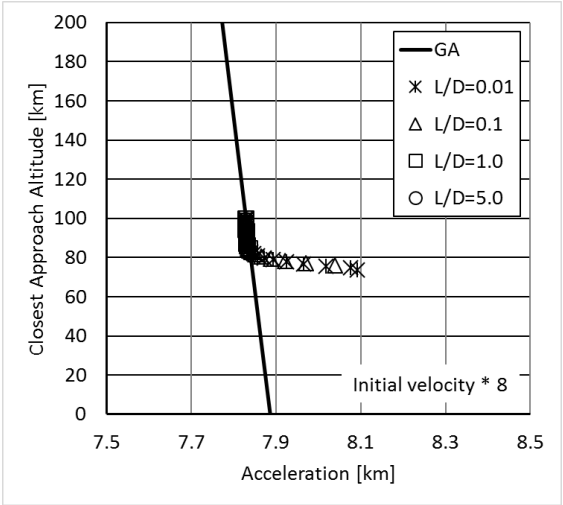

Fig. 7. Relationship between the closest altitude and acceleration (speed multiple 8)

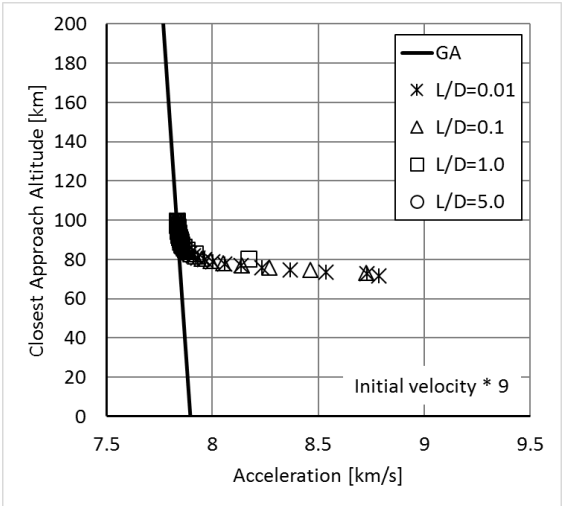

Fig. 8. Relationship between the closest altitude and acceleration (speed multiple 9)

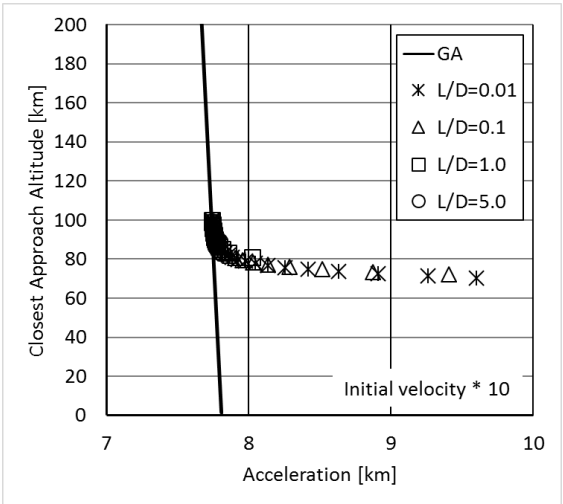

Fig. 9. Relationship between the closest altitude and acceleration (speed multiple 10)

Fig. 10 shows the relationship between the closest approach altitude and acceleration obtained by the aero-gravity assist calculation, in which the initial approach speeds are multiples of 10. The roll angle is 0°. Comparing Figs. 9 and 10, there is no big difference in trend. However, normal flight has better sensitivity to altitude.

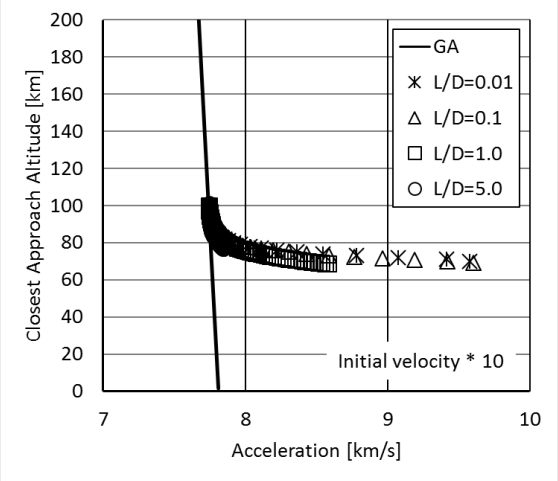

Fig. 10. Relationship between the closest altitude and acceleration (speed multiple 10, normal flight)

Tables 2 and 3 show the maximum acceleration at each lift-to-drag ratio. The speed multiple is 10 (approximately 85 at Earth arrival C3). The roll angle is -180° (upside-down flight) and 0° (normal flight), respectively. In the case where acceleration to gravity assist is 1 km/s or more as a threshold, aero-gravity assist is superior only when the lift drag ratios are 0.1 and 0.01. When comparing upside-down flight and normal flight, acceleration of normal flight is slightly larger.

Table 2. Maximum acceleration (roll: -180°)

L/D	5.0	1.0	0.1	0.01
C/A km (Design)	94	85	74	71
C/A km (Result)	89.24	80.91	72.02	70.48
ΔVkm/s (vs. GA)	7.79 (0.05)	8.02 (0.28)	9.41 (1.66)	9.60 (1.86)
Temp. °C	1857	2223	2567	2626

Table 3. Maximum acceleration (roll: 0°)

L/D	5.0	1.0	0.1	0.01
C/A km (Design)	40	40	67	70
C/A km (Result)	77.23	68.66	69.3	69.92
ΔVkm/s (vs. GA)	7.84 (0.10)	8.58 (0.84)	9.60 (1.86)	9.58 (1.83)
Temp. °C	2447	2790	1681	2645

The width of the entry corridor (altitude, kilometers) at the speed multiple 10 is shown in Table 4. The result is that acceleration with respect to gravity assist is 1 km/s or more. In addition, an integer indicates the design altitude, and the inside of the parentheses indicates the calculation result. The width of the entry corridor is very thin. The width of the entry corridor is slightly wider for normal flight than for upside-down flight.

Table 4. Entry corridor width

L/D		0.1	0.01
Width km	upside down	1 (1.39)	2 (2.15)
	normal	4 (3.12)	3 (3.03)

5. Conclusions

In this study, the effectiveness of aero-gravity assist flight with the Earth 's atmosphere was verified using three-degree-of-freedom flight analysis. As a result, the following knowledge was obtained.

- In the case of lift-to-drag ratios of 0.1 and 0.01, and a speed multiplier of 10 (approximately 85 at Earth arrival C3), the acceleration obtained by aero-gravity assist exceeds 1 km/s with respect to that of gravity assist.
- If the lift-to-drag ratio is less than 5.0, gravity aerodynamic assist is advantageous.
- The amount of acceleration obtained for normal flight is greater for upside-down flight, and the width of the entry corridor is larger.
- In the case where the initial speed is 10 times and normal flight, the width of the entry corridor is 3.13 km.

Acknowledgments

The results of this analysis were obtained by using the automatic grid generation software HexaGrid and the fast fluid analysis software FaSTAR owned by the Japan Aerospace Exploration Agency.

We would like to thank Editage (www.editage.jp) for English language editing.

References

1). M. J. Lewis and A. D. McRonald, Design of Hypersonic Waveriders for Aeroassisted Interplanetary Trajectories, Journal of Spacecraft and Rockets, Vol. 29, No. 5, 1992, pp. 653-660.

2). R. W. Detra, N. H. Kemp and F. R. Riddell, JET PROPULSION, Dec. 1957, p. 1256.

3). A. Hashimoto, K. Murakami, T. Aoyama, K. Ishiko, M. Hishida, M. Sakashita, P. Lahur, Toward the Fastest Unstructured CFD Code 'FaSTAR', AIAA-2012-1075.